Journal of Innovative Optical Health Sciences
Vol. 7, No. 2 (2014) 1330007 (11 pages)

DOI: 10.1142/S1793545813300073

World Scientific
www.worldscientific.com

A review of synthetic methods for the production of upconverting lanthanide nanoparticles

Christian F. Gainer and Marek Romanowski*
Department of Biomedical Engineering
University of Arizona
Tucson, AZ
**marekrom@email.arizona.edu*

Received 31 July 2013
Accepted 21 September 2013
Published 26 November 2013

Upconverting lanthanide nanoparticles overcome many of the problems associated with more traditionally used luminescent contrast agents, such as photobleaching, autofluorescence, cytotoxicity and phototoxicity. For this reason, they are an attractive choice for biomedical imaging applications, particularly for imaging in living tissues. The last decade has seen numerous improvements to these nanocrystals, but a comprehensive guide to the synthesis of upconverting lanthanide nanoparticles has not yet been written. Methods vary from paper to paper and from group to group, and results vary between research groups for each method. For this reason, development of these nanoparticles remains a significant endeavor for any research group interested in joining the field. In this review, we look at the varying synthetic methods employed over the last decade and detail methodology for a select few that have been favored in the field.

Keywords: Rare earth; nanocrystals; upconversion; imaging; luminescence.

1. Introduction

Upconverting lanthanide nanoparticles are a subset of luminescent contrast agents that use rare earth metals doped into a crystalline host to generate unique optical properties that make them superior to more traditionally used luminescent agents for a number of biomedical imaging applications. The most striking feature of these nanoparticles is their bright upconversion luminescence upon excitation at 980 nm (see Fig. 1). This anti-Stokes shifted emission is not shared by biological autofluorescence processes, effectively eliminating background signal from endogenous fluorophores. Furthermore, NIR excitation achieves a greater depth of penetration than visible or UV, and is less phototoxic.[1,2] Because upconverting nanoparticle (UCNP) luminescence is the result of electronic transitions within individual metal ions, it is not subject to photobleaching.[3] In addition, because each nanoparticle contains a large number of active ions, fluorescence intermittency is averaged out enough that it is not

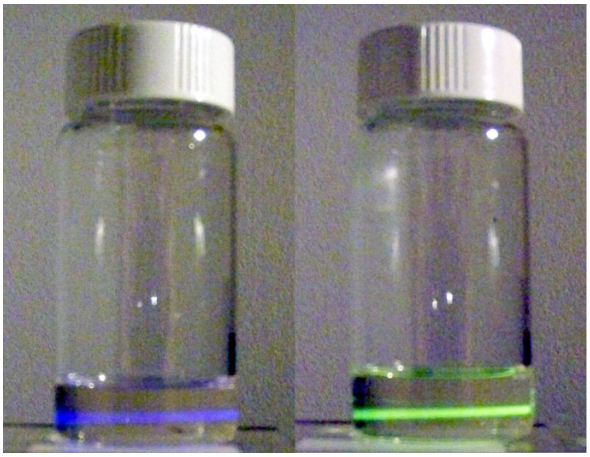

Fig. 1. $NaYF_4$ nanocrystals codoped with Yb^{3+} and Tm^{3+} (left) or Er^{3+}(right). UCNPs shown here were synthesized by thermal decomposition of LnTFA precursors, and had an average diameter of ∼15 nm. Illumination was by laser diode at 980 nm.

observed for single particles.[4–7] For these reasons, UCNPs have been pursued as contrast agents for biomedical imaging during the past decade.[8–11] They are not, however, without disadvantages. Of primary concern is the low upconversion efficiency of the base nanoparticles when compared to the downconversion luminescence of fluorescent dyes.[12] Typical quantum yields for $NaYF_4$:Yb, Er range from 0.005% to 3%, with 3% representing the quantum yield of the bulk material.[13] In general, the quantum yield of UCNPs increases with increasing size. Quantum yield is also affected by the number of defect sites on the surface of the nanoparticle, the capping ligand used to stabilize UCNPs in solution, the solvent and the crystal phase of the nanoparticles.[10] With so many variables, the synthesis of UCNPs has been constantly evolving to achieve better control of luminescence, particle size and colloidal stability. In this paper, we review UCNP synthetic methods developed over the last decade and describe several specific protocols in order to create a single, open source reference for many of the techniques used in UCNP synthesis.

The first report of a synthetic method for producing stable suspensions of upconverting lanthanide nanoparticles was published in 2003 by Heer *et al.*[14] Before that time, upconverting lanthanide materials were typically synthesized as phosphors, bulk materials,[15–17] or dry nanoparticles that could not be dispersed in solution.[18–20] The nanoparticles synthesized by Heer at that time had an average diameter of ∼7 nm and were composed of $YbPO_4$:$Er_{0.05}$ and $LuPO_4$:$Yb_{0.49}$, $Tm_{0.01}$. Due to the host material chosen, the upconversion efficiency of these nanoparticles was low, though upconversion luminescence could still be observed with naked eye. Shortly after this was published, Heer *et al.* released a second paper describing the synthesis of highly efficient upconverting lanthanide nanoparticles, choosing $NaYF_4$ as the host matrix instead of the previously used phosphates.[21] The switch from phosphate crystal lattices to $NaYF_4$ was accompanied by an eight-fold increase in the luminescence intensity of UCNPs. The authors make sure to clarify that this increase in luminescence efficiency is not solely due to the change in the host lattice. Particle size was also noted to increase substantially between the particles composed of $YbPO_4$ and those composed of $NaYF_4$, resulting in a decrease in the relative number of lanthanide ions available for surface quenching effects. In addition, they posited that the decrease in the amount of Yb^{3+} reduced quenching effects caused by this ion.

Since these seminal papers on the synthesis of UCNPs, there has been a dramatic increase in activity in this field. There are now many techniques available for the synthesis of upconverting nanocrystals, each with its own advantages and disadvantages.

2. Synthetic Methods

Before discussing individual synthetic methods, it is necessary to discuss the various factors that determine UCNP quality during synthesis. The first, and most important, is the choice of sensitizer and activator ions. Most UCNPs take advantage of energy transfer upconversion in order to generate upconverted luminescence. The sensitizer absorbs excitation light, then transfers that energy nonradiatively to a nearby activator. Following multiple energy transfer or direct excitation events, the activator builds up enough energy to emit energy at a shorter wavelength than the excitation source. In most cases, Yb^{3+} is chosen as the sensitizer due to its single, relatively strong transition in the visible/NIR spectrum. In addition, the $^2F_{7/2} \rightarrow {}^2F_{5/2}$ transition matches several electronic transitions in Er^{3+}, Tm^{3+} and Ho^{3+} very well (see Fig. 2). The doping ratio of the sensitizer is critical. It must be high enough that the average distance

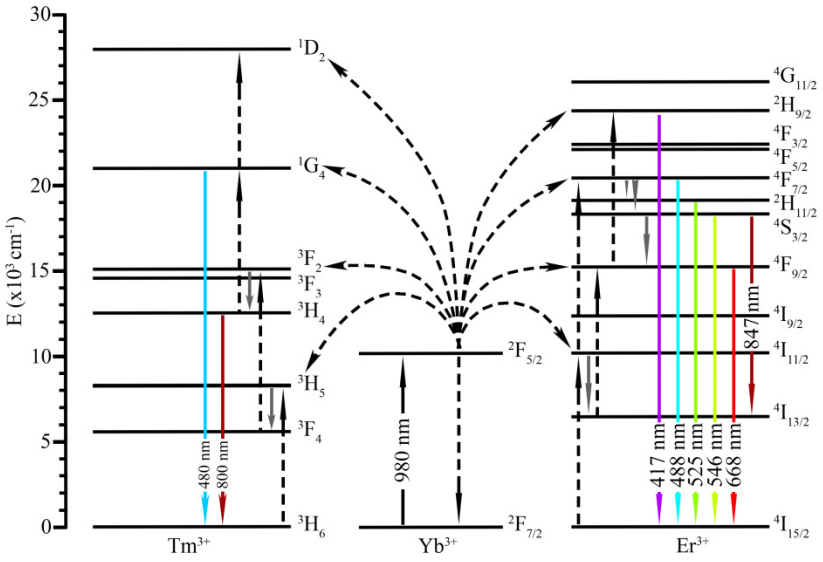

Fig. 2. Energy level diagram for energy transfer upconversion in $NaYF_4$:Yb^{3+}, Tm^{3+} and $NaYF_4$:Yb^{3+}, Er^{3+}. Dashed lines represent energy transfer excitation and relaxation, gray lines represent nonradiative relaxation, and colored lines represent radiative transitions. Energy levels taken from Carnall *et al.*[23,24]

between sensitizers and activators favors energy transfer, but not so high that cross-relaxation, cooperative luminescence or rapid energy diffusion between sensitizers results in significant upconversion quenching.[10,21,22] As mentioned, typical activators are Er^{3+}, Tm^{3+} and Ho^{3+} due to the resonance match with Yb^{3+}. In a more general sense, good activators will have long-lived intermediate excited states. The longer an electron spends in an excited metastable intermediate, the more likely it is to be excited again by an incident photon or by energy transfer from a nearby ion. In addition, those activators that have multiple transitions with similar energy gaps make good dopants for upconverting materials. For example, Er^{3+} has more than four transitions that have energies close to 10,200 cm^{-1} (980 nm). This enhances both single wavelength excited state absorption (ESA) and ETU.

Second to a proper sensitizer/activator combination is the host matrix. As already mentioned in the context of $NaYF_4$ and $YbPO_4$, choosing a good host matrix can greatly enhance upconversion efficiency.[21] There are four major considerations for these crystal matrices. The first is size matching between matrix cations and the lanthanide ions. Because trivalent lanthanide ions all possess very similar ionic sizes and chemical properties, they are ideal as inactive host matrix cations. This is particularly true with Y^{3+}, Gd^{3+} and La^{3+} as they do not have strong electronic transitions in the visible and NIR, though the latter has a few strong transitions in the UV and violet wavelengths.[25] Alkaline earth metals and some transition metals also have similar ionic size to the lanthanide ions. These include Ca^{2+}, Ba^{2+}, Sr^{2+}, Zr^{4+} and Ti^{4+}. However, due to the charge mismatch, crystals composed of these materials often have numerous defects when doped with lanthanide ions.[10]

Lattice phonon energy is also of great importance in selecting a host matrix for upconverting materials. Its influence on the nonradiative transition rate, k_{nr}, can be expressed as

$$k_{nr} = \beta e^{-\alpha(\Delta E - 2\hbar\omega)} \quad (1)$$

for low phonon numbers and

$$k_{nr} = \beta e^{-\alpha(\Delta E)} \quad (2)$$

for phonon numbers above two or three, where β and α are constants unique to each host matrix, ΔE is the energy gap between the two electronic states of interest, and $\hbar\omega$ is the maximum phonon energy for the host matrix.[26] Oxide nanocrystals have the largest phonon energies among those considered for UCNPs, typically between 550 and 700 cm^{-1}, while halogen-based nanoparticles range from 175 cm^{-1} for $LaBr_3$ to ~350 cm^{-1} for $NaYF_4$. While host matrices based on bromine and iodine seem like obvious choices based on their phonon energies, they do not have good stability in biological environments. Matrices composed with Br^- and I^-

are hygroscopic and not well suited for use in biological systems. $NaYF_4$ is relatively stable in aqueous media, however, and is therefore ideal for the purpose of developing UCNPs as biomedical contrast agents.

In addition to the chemical composition of the nanocrystal, crystal lattice structure is important when creating efficient upconverting materials. $NaYF_4$ nanocrystals may be either cubic (α-$NaYF_4$) or hexagonal (β-$NaYF_4$) phase, with the hexagonal phase nanoparticles typically being an order of magnitude more efficient at photon upconversion.[27] Unfortunately, synthesis of hexagonal phase nanoparticles is often significantly more difficult than synthesis of their cubic phase counterparts, requiring higher reaction temperatures and strict control of most other reaction parameters.

Finally, the capping ligand used to stabilize the UCNPs in solution has a direct effect on upconversion efficiency. Vibrational modes of the capping ligand will interact with surface ions, often resulting in quenching of their luminescence. This occurs alongside solvent quenching and can be mitigated by the epitaxial growth of additional $NaYF_4$ or $NaGdF_4$ to form a shell around the active core.[28–30] With these properties in mind, we now look at each synthetic method in detail and weigh their pros and cons.

2.1. *Thermal decomposition*

Arguably the most popular method of UCNP synthesis over the past decade has been thermal decomposition.[50–55] Thermal decomposition involves the heating of lanthanide precursors in nonpolar solvents with high boiling points in the presence of other host matrix materials. A capping ligand is usually used to manage nanoparticle growth and stabilize the growing nanoparticles in solution. In many of the current thermal decomposition methods reported, oleic acid is used in conjunction with either oleylamine or trioctylphosphine. Because of the high temperatures involved and the general sensitivity of UCNPs to oxygen impurities, control over the reaction must be precise in order to produce good-quality nanocrystals of a narrow monodisperse size. Parameters that influence nanocrystal morphology, size and crystal phase include temperature, pressure, capping ligand, precursor composition, heating rate, cooling rate, reaction time, solvent and reagent concentrations.[56] Careful selection of these parameters allows for control over UCNP size and crystal phase. However, the large number of variables can make reproducible synthesis exceptionally challenging. While thermal decomposition produces good UCNPs, it also produces toxic byproducts. As such, a number of groups have pursued alternative synthetic methods.

There are two major techniques for the formation of UCNPs by thermal decomposition, as well as a small number of less used techniques. Before going into the details of these methods, it should first be reiterated that thermal decomposition methods usually produce fluorinated byproducts that are extremely hazardous. In addition, the biological effects of UCNPs are still being studied, and though initial experiments indicate that they are fairly nontoxic, precautions should still be taken to ensure that all synthetic work and handling of UCNPs takes place in a fume hood with proper protective equipment.

In the first synthetic method we will describe the thermal decomposition of lanthanide oleate precursors, often carried out as a one-pot reaction. This technique was first proposed by Li and Zhang in 2008, and has been used and further developed by several groups since.[28,51,53] The reaction begins by adding 1 mmol of lanthanide salts, one study found that lanthanide acetates work particularly well, into a flask along with 6 mL oleic acid and 17 mL 1-octadecene. The lanthanide salts are usually added at a molar ratio of 2% Er^{3+} or 0.2% Tm^{3+}, 20–30% Yb^{3+} and the remainder Y^{3+} or Gd^{3+}. The concentration of oleic acid has been reported to influence particle size, with higher concentrations of oleic acid resulting in smaller particles.[53] The resulting suspension is stirred and heated to 120–160°C under vacuum, and held at this temperature between 30 min and 1 h. In our own work, we found that alternating between Ar atmosphere and vacuum during the first 100°C of any heating step resulted in a better end product. Completion of this step is marked by transition from a cloudy suspension to a transparent solution. At this point, the solution is cooled between room temperature and 50°C. In our own use of this protocol, we found no difference between 25°C and 50°C, though more trials are needed to establish this conclusively. About 10 mmol of NaOH and 5 mmol of NH_4F are then dissolved in 10 mL of MeOH, which is added to the reaction flask. We did not find any significant

correlation between UCNP quality and the rate at which this solution is added to the reaction mixture. There have been reports that increasing the concentration of sodium above the stoichiometric concentration has beneficial effects on UCNP quality, which is why NaOH is added at 10 times the stoichiometric concentration. The resulting slurry is typically colorless to light yellow and cloudy. The slurry is then heated to 100°C under vacuum to remove water and MeOH from the reaction flask. Once these have been removed, the reaction vessel is placed under Ar atmosphere and rapidly heated to 310°C, then held at this temperature for between 0.5 and 1.5 h. The resulting suspension of nanoparticles is then cooled to room temperature, at which point ethanol or acetone may be used to precipitate particles from solution and wash them. The results of this synthetic protocol have varied between research groups. While the original authors of this method and several of the immediately following publications by other groups report hexagonal phase nanoparticles, some groups also report cubic phase nanoparticles as a result of this method. In our own work, each synthesis using this method resulted in a mixture of small (<100 nm) cubic phase particles and large (>200 nm) hexagonal phase particles. The ratio of small to large particles varied between each synthesis.

The second method, first described by Boyer *et al.* in 2006, is the thermal decomposition of lanthanide trifluoroacetate precursors.[50,57] To begin, lanthanide oxides are dissolved in 50% trifluoroacetic acid at 80°C. This often takes overnight, sometimes longer, and is marked by a transition from a cloudy suspension to a transparent colorless solution. The resulting solution is then dried. In our own work, we then dissolve the precursors in tertiary butanol, lyophilize them and store them for later use. About 1 mmol of these precursors are then added to 10 mmol oleic acid, 10 mmol oleylamine and 20 mmol 1-octadecene along with 1 mmol sodium trifluoroacetate. The solution is then heated to 100°C and left at this temperature under vacuum pressure for 1 h. After an hour, the solution is rapidly heated to 270°C and maintained at this temperature for another hour. The suspension is then cooled to room temperature and ethanol or acetone is added to precipitate and wash the nanoparticles. The UCNPs are cubic phase nanocrystals at this point, and can be run through a second heat treatment to promote a transition from cubic to hexagonal phase. This is done by first dispersing the washed, dried UCNPs in 20 mmol oleic acid and 20 mmol 1-octadecene along with sodium trifluoroacetate. The resulting slurry is then heated to 100°C with magnetic stirring and held at this temperature for 1 h under vacuum pressure. The solution is then heated to 330°C and held at this temperature for 15 min before cooling to room temperature and precipitating and washing the UCNPs with ethanol or acetone.

In the third thermal decomposition method we will discuss the review of the hot injection method.[4,58] To begin, lanthanide trifluoroacetate precursors are prepared as described previously. About 1.25 mmol of sodium trifluoroacetate and 1.25 mmol lanthanide trifluoroacetates are then added to 2.5 mL of 1-octadecene and 5 mL of oleic acid. To a three-neck round bottom flask, 15 mL of 1-octadecene and 10 mL of oleic acid are added. Both solutions are then heated to 125°C under vacuum and maintained at this temperature with stirring for 30 min to remove residual water and oxygen. The three-neck flask is then heated to 310°C under argon. At this time, the solution containing the lanthanide trifluoroacetates is added dropwise to the three-neck flask. Once added, the reaction vessel was cooled to 305°C and held at this temperature for 20 min, then cooled to room temperature. The sample is purified as described previously.

In all of the above cases, the luminescence yield of the synthesized UCNPs can be substantially improved by the epitaxial growth of a shell layer onto the nanocrystal core. This typically uses a method similar to the three methods described above, but with some slight modification.[51] In most cases, the growth of a shell layer is accomplished by repeating one of the protocols outlined above with some small modifications. Core nanoparticles are added to the reaction vessel alongside the lanthanide precursors, and the concentrations of the various lanthanide ions are altered to modify the size and composition of the shell layer. Undoped $NaYF_4$ and $NaGdF_4$ are common crystal compositions for UCNP shells.

2.2. *Coprecipitation*

Compared to thermal decomposition, coprecipitation is a very friendly synthetic method. Not only are there fewer toxic byproducts, but the temperatures required during the initial synthesis are not

as extreme.[59] Unfortunately, these factors are outweighed by lower UCNP quality immediately following synthesis, often requiring additional annealing to achieve good photon upconversion.[10] An example synthesis involves the rapid injection of a lanthanide-EDTA complex into a solution made up of NaF in deionized water, resulting in immediate nucleation. This is then allowed to react at room temperature for 1 h. Following precipitation by centrifugation and several wash steps, the dry nanoparticles may be annealed at 400°C to promote the transition from cubic to hexagonal phase.[60]

Alternatively, polyvinylpyrrolidone (PVP) may be used as the surface ligand. The following coprecipitation procedure was taken from work by Li and Zhang in 2006.[61] To begin, 1 mmol of Ln_2O_3 is dissolved in 10% HNO_3 and the resulting solution is heated to remove water. The resulting $LnNO_3$ salts are dissolved in 10 mL of ethylene glycol. About 0.5560 g PVP40 and 0.0588 g NaCl are added to the reaction vessel, and the resulting mixture is heated to 80°C until a homogenous solution is formed. About 4 mmol of NH_4F is then dissolved in 10 mL ethylene glycol at 80°C, which is then added to the solution containing $LnNO_3$ dropwise. The resulting solution is stirred at 80°C for 10 min before being heated to 160°C. The solution is maintained at this temperature for 2 h, then cooled to room temperature. The resulting UCNPs are precipitated from solution and washed with ethanol.

2.3. *Solvothermal*

Along the same lines as coprecipitation, solvothermal synthetic techniques require lower temperatures and produce fewer toxic byproducts than thermal decomposition methods. The main requirement for solvothermal synthesis is an autoclave, which is necessary in order to bring the polar solvents used to temperatures and pressures above their critical points.[54,62] Organic solvents may be added to these reactions to help control crystal growth and directionality, though high-quality nanoparticles can still be synthesized without them.[39]

The following protocol has been taken from work by Wang *et al.* and details the generation of CaF_2: Yb, Er nanocrystals.[63,64] To begin, stock solutions of $YbCl_3$ and $ErCl_3$ are prepared by dissolving LnO_3 salts in dilute hydrochloric acid. About 0.5 mmol of the $Ln(Ca)Cl_3$ salts and 4 mL of 0.5 M NaF is added to a mixture of NaOH (1.2 g), ethanol (8 mL), deionized water (8 mL) and oleic acid (20 mL). The resulting suspension is stirred, then added to a 50 mL Teflon-lined autoclave and maintained at 180°C for 36 h. The product is then allowed to cool to room temperature, collected by centrifugation and washed with ethanol. To create $NaYF_4$ nanocrystals, $CaCl_2$ is replaced with YCl_3 and additional NaF, between 2 and 6 mmol, is added.[65]

An example of a hydrothermal synthesis that does not utilize organic solvents was presented by Passuello *et al.* in 2012 and is detailed here.[43] To begin, $YbCl_3$, $GdCl_3$, and either $ErCl_3$ or $TmCl_3$ are dissolved in 17 mL of deionized water to achieve a lanthanide concentration of 0.124 M at a molar ratio of 78% Gd^{3+}, 20% Yb^{3+} and 2% Er^{3+} or Tm^{3+}. NH_4F is then added to the solution to a concentration of 0.372 M along with enough PEG-10,000 to achieve a water:PEG mass ratio of 1. The resulting suspension is placed in a 100 mL Teflon-lined digestion pressure vessel and maintained at 200°C for 8 h. Following synthesis, the nanoparticles are washed with acetone and dried at room temperature, then dispersed in water.

Other, less well known, synthetic methods include ionothermal,[66] sol–gel,[67] combustion[68] and flame synthesis.[69] Flame synthesis is particularly enticing due to its scalability and low cost, though additional work is necessary to refine the technique. While each of these synthetic methods has its own virtues, for biomedical applications, the nanoparticles produced are in general inferior to thermal decomposition and solvothermal methods.

3. Surface Modification and Future Directions

As can be seen in Table 1, the UCNPs created by many of available synthetic methods are hydrophobic as synthesized. For this reason, surface modification is considered essential for most biomedical applications. In addition to hydrophilicity, surface functionality is also an often sought after goal in UCNP surface modification. Common functional groups include amines, thiols and carboxylic acids due to the ease with which they may be reacted with many biologically relevant molecules. Functionalization with maleimide has also been proposed recently as a convenient method for the attachment of proteins.[70] For simplicity, surface modification methods investigated so far can

Table 1. Recent results for nanoparticle synthesis from selected papers.

Synthetic method	H_2O dispersible	Precursor	Surface ligand	Particle diameter	Reaction temperature	Crystal phase	Host matrix	Reference
Thermal Decomposition	No	LnTFA	Oleic acid	23 nm	305°C	Cubic	$NaYF_4$	31
Thermal Decomposition	No	LnOleate	Oleic acid	10.5 nm	280°C	Hexagonal	$NaGdF_4$	32
Thermal Decomposition	No	LnOleate	Oleic acid	12.2 nm	300°C	Tetragonal	$BaYF_5$	33
Thermal Decomposition	No	LnOleate	Oleic acid	45 nm/8 nm	320°C	Hexagonal/Cubic	$NaY(Mn)F_4$	34
Thermal Decomposition	No	$Ln_2(CO_3)_3$	Oleic acid	65 nm	310°C	Hexagonal	$NaYF_4$	35
Thermal Decomposition	No	LnOleate	Oleic acid	26 nm	300°C	Hexagonal	$NaYF_4$	36
Thermal Decomposition	No	LnOleate	Oleic acid	90 nm	300°C	Hexagonal/Cubic	$NaYF_4$	37
Solvothermal	Yes	$LnCl_3$	Citric acid	11 nm	190°C	Cubic	CaF_2	38
Solvothermal	No	$LnCl_3$	Oleic acid	20 nm	200°C	Cubic	$NaY(Mn)F_4$	39
Solvothermal	Yes	$Ln(NO_3)_3$	Citric acid	40 nm	200°C	Tetragonal	YVO_4	40
Solvothermal	Yes	$LnCl_3$	PEI	55 nm	200°C	Hexagonal	$NaYF_4$	41
Solvothermal	Yes	$LnCl_3$	PEG	5 nm	160°C	Cubic	$NaYF_4$	42
Solvothermal	Yes	$LnCl_3$	PEG	65 nm	200°C	Orthorhombic	GdF_3	43
Solvothermal	No	$Ln(NO_3)_3$	Oleic acid	13 nm	220°C	Cubic	$SrYbF_5$	44
Solvothermal	No	$LnCl_3$	Oleic acid	10 nm	160°C	Cubic	$BaYbF_5$	45
Solvothermal	No	$LnCl_3$	Oleic acid	350 × 950 nm	193°C	Hexagonal	$NaYb(Gd)F_4$	46
Solvothermal	No	$LnCl_3$	Oleic acid	10 nm	200°C	—	Ba_2YF_7	47
Coprecipitation	Yes	$LnNO_3$	PVP	30 nm	160°C	Cubic	$NaYF_4$	48
Laser Ablation	Yes	Y_2O_3:Yb, Er	NA	11 nm	NA	Cubic	Y_2O_3	49

be roughly divided into five categories: ligand exchange,[55,71–74] ligand modification,[75,76] ligand removal,[52] adsorption of amphiphilic molecules[4,5,77–80] and growth of a silica shell.[81,82] From our experience, coating with amphiphilic molecules is the simplest surface modification method both for dispersing UCNPs in aqueous solutions and for functionalization with biologically relevant ligands. The true test of these nanoparticles will be in their application, however, and more study of surface modification's effect on toxicity, biodistribution and functionality is needed.

In order to better study biomedical application of UCNPs, more reproducible synthetic methods are necessary. Small changes in nanoparticle size can have dramatic effects on nanoparticle distribution in live animals, colloidal stability and upconversion efficiency.[83] To that end, automated and large-scale synthesis are areas that warrant additional study.[84]

Most laboratories studying UCNP synthesis or biomedical application now focus on thermal decomposition or solvothermal methods. Despite challenging preparative conditions, these methods are preferred for their ability to produce high-quality nanoparticles that have a monodisperse size, pure crystal phase, protective shell layers and relatively high upconversion efficiency.

Control of UCNP size, crystal structure, quantum yield and surface functionality still present a considerable experimental challenge. The large number of protocols tested has not led to a standard synthetic method. On the contrary, as evidenced by continuing reports of new synthetic approaches, nanocrystal compositions and surface modifications, UCNP synthesis remains a very active field of research.

Acknowledgment

The authors acknowledge financial support for this research by the National Institutes of Health (CA120350) and the National Science Foundation NSF (CBET 0853921).

References

1. J. M. Squirrell, D. L. Wokosin, V. E. Centonze, J. G. White, B. D. Bavister, "Mitochondrial dynamics of living hamster embryos imaged by two-photon excitation," *Mol. Biol. Cell.* **7**(S), 3748–3748 (1996).
2. J. Zhou, Z. Liu, F. Li, "Upconversion nanophosphors for small-animal imaging," *Chem. Soc. Rev.* **41**, 1323–1349 (2012).
3. D. K. Chatterjee, A. J. Rufaihah, Y. Zhang, "Upconversion fluorescence imaging of cells and small animals using lanthanide doped nanocrystals," *Biomaterials* **29**(7), 937–943 (2008).
4. Y. I. Park, S. H. Nam, J. H. Kim, Y. M. Bae, B. Yoo, H. M. Kim, K. S. Jeon, H. S. Park, J. S. Choi, K. T. Lee, Y. D. Suh, T. Hyeon, "Comparative study of upconverting nanoparticles with various crystal structures, core/shell structures, and surface characteristics," *J. Phys. Chem. C* **117**(5), 2239–2244 (2013).
5. Y. I. Park, J. H. Kim, K. T. Lee, K. S. Jeon, H. B. Na, J. H. Yu, H. M. Kim, N. Lee, S. H. Choi, S. I. Baik, H. Kim, P. S. Park, B. J. Park, Y. W. Kim, S. H. Lee, S. Y. Yoon, I. C. Song, W. K. Moon, Y. D. Suh, T. Hyeon, "Nonblinking and nonbleaching upconverting nanoparticles as an optical imaging nanoprobe and T1 magnetic resonance imaging contrast agent," *Adv. Mater.* **21**(44), 4467–4471 (2009).
6. S. Wu, G. Han, D. J. Milliron, S. Aloni, V. Altoe, D. V. Talapin, B. E. Cohen, P. J. Schuck, "Nonblinking and photostable upconverted luminescence from single lanthanide-doped nanocrystals," *Proc. Natl. Acad. Sci. USA* **106**(27), 10917–10921 (2009).
7. A. D. Ostrowski, E. M. Chan, D. J. Gargas, E. M. Katz, G. Han, P. J. Schuck, D. J. Milliron, B. E. Cohen, "Controlled synthesis and single-particle imaging of bright, sub-10 nm lanthanide-doped upconverting nanocrystals," *ACS Nano* **6**(3), 2686–2692 (2012).
8. H. H. Gorris, O. S. Wolfbeis, "Photon-upconverting nanoparticles for optical encoding and multiplexing of cells, biomolecules, and microspheres," *Angew. Chem. Int. Ed.* **52**, 2–19 (2013).
9. M. Haase, H. Schafer, "Upconverting Nanoparticles," *Angew. Chem. Int. Ed.* **50**, 2–24 (2011).
10. F. Wang, X. Liu, "Recent advances in the chemistry of lanthanide-doped upconversion nanocrystals," *Chem. Soc. Rev.* **38**, 976–989 (2009).
11. Y. Liu, H. Zhu, X. Chen, "Lanthanide-dopeed luminescent nanoprobes: Controlled synthesis, optical spectroscopy, and bioapplications," *Chem. Soc. Rev.* **42**, 6924–6958 (2013).
12. F. C. van Veggel, C. Dong, N. J. J. Johnson, J. Pichaandi, "Ln^{3+}-doped nanoparticles for upconversion and magnetic resonance imaging: Some critical notes on recent progress and some aspects to be considered," *Nanoscale* **4**(23), 7309–7321 (2012).
13. J. C. Boyer, F. C. J. M. van Veggel, "Absolute quantum yield measurements of colloidal NaYF4:

Er^{3+}, Yb^{3+} upconverting nanoparticles," *Nanoscale* **2**, 1417–1419 (2010).
14. S. Heer, O. Lehmann, M. Haase, H. U. Gudel, "Blue, green, and red upconversion emission from lanthanide-doped $LuPO_4$ and $YbPO_4$ nanocrystals in a transparent colloidal solution," *Angew. Chem. Int. Ed.* **42**(27), 3179–3182 (2003).
15. E. Downing, L. Hesselink, J. Ralston, R. Macfarlane, "A three-color, solid-state, three-dimensional display," *Science* **273**(5279), 1185–1189 (1996).
16. W. Lenth, R. M. Macfarlane, "Excitation mechanisms for upconversion lasers," *J. Lumin.* **45**(1–6), 346–350 (1990).
17. N. Bloembergen, "Solid state infrared quantum counters," *Phys. Rev. Lett.* **2**(3), 84–85 (1959).
18. D. Matsuura, "Red, green, and blue upconversion luminescence of trivalent-rare-earth ion-doped Y2O3 nanocrystals," *Appl. Phys. Lett.* **81**(24), 4526–4528 (2002).
19. B. Sun, G. Yi, F. Yang, D. Chen, Y. Zhou, J. Cheng, "Synthesis and characterization of high-efficiency nanocrystal up-conversion phosphors: Ytterbium and erbium codoped lanthanum molybdate," *Chem. Mater.* **14**(7), 2910–2914 (2002).
20. J. A. Capobianco, J. C. Boyer, F. Vetrone, A. Speghini, M. Bettinelli, "Optical spectroscopy and upconversion studies of Ho^{3+}-doped bulk and nanocrystalline Y_2O_3," *Chem. Mater.* **14**(7), 2915–2921 (2002).
21. S. Heer, K. Kompe, H. U. Gudel, M. Haase, "Highly efficient multicolour upconversion emission in transparent colloids of lanthanide-doped $NaYF_4$ nanocrystals," *Adv. Mater.* **16**(23–24), 2102–2105 (2004).
22. F. Auzel, "Upconversion and anti-stokes processes with f and d ions in solids," *Chem. Rev.* **104**(1), 139–174 (2004).
23. W. T. Carnall, G. L. Goodman, K. Rajnak, R. S. Rana, "A systematic analysis of the spectra of the lanthanides doped into single crystal LaF_3," *J. Chem. Phys.* **90**(7), 3443–3457 (1989).
24. W. T. Carnall, H. Crosswhite, "Further interpretation of the spectra of Pr^{3+}-LaF_3 and Tm^{3+}-LaF_3*," *J. Less-Common Met.* **93**, 127–135 (1983).
25. J. Reader, C. H. Corliss, "Line spectra of the elements," in *Handbook of Chemistry and Physics*, E-217–E-349, Boca Raton, CRC Press, Inc. (1979).
26. J. M. F. van Dijk, M. F. H. Schuurmans, "On the nonradiative and radiative decay rates and a modified exponential energy gap law for 4f-4f transitions in rare earth ions," *J. Chem. Phys.* **78**(9), 5317–5323 (1983).
27. K. W. Kramer, D. Biner, G. Frei, H. U. Gudel, M. P. Hehlen, S. R. Luthi, "Hexagonal sodium yttrium fluoride based green and blue emitting upconversion phosphors," *Chem. Mater.* **16**, 1244–1251 (2004).
28. H. S. Qian, Y. Zhang, "Synthesis of hexagonal-phase core-shell $NaYF_4$ nanocrystals with tunable upconversion fluorescence," *Langmuir* **24**, 12123–12125 (2008).
29. G. S. Yi, G. M. Chow, "Water-soluble $NaYF_4$:Yb, Er(Tm)/$NaYF_4$/polymer core/shell/shell nanoparticles with significant enhancement of upconversion fluorescence," *Chem. Mater.* **19**(3), 341–343 (2007).
30. F. Vetrone, R. Naccache, V. Mahalingam, C. G. Morgan, J. A. Capobianco, "The active-core/active-shell approach: A strategy to enhance the upconversion luminescence in lanthanide-doped nanoparticles," *Adv. Funct. Mater.* **19**(18), 2924–2929 (2009).
31. K. Prorok, A. Gnach, W. Strek, "Energy up-conversion in Tb^{3+}/Yb^{3+} co-doped colloidal alpha-$NaYF_4$ nanocrystals," *J. Lumin.* **140**, 103–109 (2013).
32. F. Liu, X. He, H. You, H. Zhang, Z. Wang, "Conjugation of $NaGdF_4$ upconverting nanoparticles on silica nanospheres as contrast agents for multi-modality imaging," *Biomaterials* **34**(21), 5218–5225 (2013).
33. L. P. Jia, B. Yan, Q. Zhang, "Barium rare earth fluoride nanocrystals: High temperature solution synthesis, characterization and luminescence," *J. Nanopart. Res.* **15**(4), 1540 (2013).
34. Z. Wu, M. Lin, S. Liang, Y. Liu, H. Zhang, B. Yang, "Hot-injection synthesis of manganese-ion-doped $NaYF_4$:Yb, Er nanocrystals with red up-converting emission and tunable diameter," *Part. Part. Syst. Char.* **30**(4), 311–315 (2013).
35. X. Luo, K. Akimoto, "Upconversion properties in hexagonal-phase $NaYF_4$:Er^{3+}/$NaYF_4$ nanocrystals by off-resonant excitation," *Appl. Surf. Sci.* **273**, 257–260 (2013).
36. J. Liu, J. Cheng, Y. Zhang, "Upconversion nanoparticle based LRET system for sensitive detection of MRSA DNA sequence," *Biosens. Bioelectron.* **43**, 252–256 (2013).
37. P. Kannan, F. A. Rahim, R. Chen, X. Teng, L. Huang, H. Sun, D. H. Kim, "Au nanorod decoration on $NaYF_4$:Yb/Tm nanoparticles for enhanced emission and wavelength-dependent biomolecular sensing," *ACS Appl. Mater. Interfaces* **5**(9), 3508–3513 (2013).
38. N. N. Dong, M. Pedroni, F. Piccinelli, G. Conti, A. Sbarbati, J. E. Ramírez-Hernández, L. M. Maestro, M. C. Iglesias-de la Cruz, F. Sanz-Rodriguez, A. Juarranz, F. Chen, F. Vetrone, J. A. Capobianco, J. G. Sole, M. Bettinelli, D. Jaque, A. Speghini, "NIR-to-NIR two-photon excited CaF_2:Tm^{3+},Yb^{3+} nanoparticles: Multifunctional nanoprobes for highly penetrating fluorescence bioimaging," *ACS Nano* **5**(11), 8665–8671 (2011).
39. C. Wang, L. Cheng, Y. Liu, X. Wang, X. Ma, Z. Deng, Y. Li, Z. Liu, "Imaging-guided pH-sensitive

photodynamic therapy using charge reversible upconversion nanoparticles under near-infrared light," *Adv. Funct. Mater.* **23**(24), 3077–3086 (2013).
40. Y. Liang, P. Chui, X. Sun, Y. Zhao, F. Cheng, K. Sun, "Hydrothermal synthesis and upconversion luminescent properties of YVO_4:Yb^{3+}, Er^{3+} nanoparticles," *J. Alloy. Compd.* **552**(9), 289–293 (2013).
41. Y. Wang, L. Ji, B. Zhang, P. Yin, Y. Qiu, D. Song, J. Zhou, Q. Li, "Upconverting rare-earth nanoparticles with a paramagnetic lanthanide complex shell for upconversion fluorescent and magnetic resonance dual-modality imaging," *Nanotechnology* **24**(17), 175101 (2013).
42. T. Cao, Y. Yang, Y. Sun, Y. Wu, Y. Gao, W. Feng, F. Li, "Biodistribution of sub-10 nm PEG-modified radioactive/upconversion nanoparticles," *Biomaterials* **34**, 7127–7134 (2013).
43. T. Passuello, M. Pedroni, F. Piccinelli, S. Polizzi, P. Marzola, S. Tambalo, G. Conti, D. Benati, F. Vetrone, M. Bettinelli, A. Speghini, "PEG-capped, lanthanide doped GdF_3 nanoparticles: Luminescent and T_2 contrast agents for optical and MRI multimodal imaging," *Nanoscale* **4**, 7682–7689 (2012).
44. L. Gong, J. Yang, Y. Li, M. Ma, C. Xu, G. Ren, J. Lin, Q. Yang, "Solvothermal synthesis and upconversion emission of monodisperse ultrasmall $SrYbF_5$ nanocrystals," *J. Mater. Sci.* **48**(10), 3672–3678 (2013).
45. H. Xing, X. Zheng, Q. Ren, W. Bu, W. Ge, Q. Xiao, S. Zhang, C. Wei, H. Qu, Z. Wang, Y. Hua, L. Zhou, W. Peng, K. Zhao, J. Shi, "Computed tomography imaging-guided radiotherapy by targeting upconversion nanocubes with significant imaging and radiosensitization enhancements," *Sci. Rep.* **3**, 1751 (2013).
46. Y. Chen, X. Yan, Q. Liu, X. Wang, "Morphology and upconversion luminescence of NaYbF4:Tm^{3+} nanocrystals modified by Gd^{3+} ions," *J. Alloy. Compd.* **562**, 99–105 (2013).
47. X. Chuai, F. Yin, Z. Liu, F. Shi, J. Wang, L. Wang, K. Zheng, C. He, W. Qin, "Tunable upconversion emission in Ba_2YF_7:Yb^{3+}/Er^{3+} nanocrystals with different Yb^{3+} concentration," *Mater. Res. Bull.* **48** (6), 2361–2364 (2013).
48. B. Sikora, K. Frone, I. Kaminska, K. Koper, S. Szewczyk, B. Paterczyk, T. Wojciechowski, K. Sobczak, R. Minikayev, W. Paszkowicz, P. Stepien, D. Elbaum, "Transport of $NaYF_4$:Er^{3+},Yb^{3+} up-converting nanoparticles into HeLa cells," *Nanotechnology* **24**(23), 235702 (2013).
49. Y. Onodera, T. Nunokawa, O. Odawara, H. Wada, "Upconversion properties of Y_2O_3:Er, Yb nanoparticles prepared by laser ablation in water," *J. Lumin.* **137**, 220–224 (2013).
50. J. C. Boyer, F. Vetrone, L. A. Cuccia, J. A. Capobianco, "Synthesis of colloidal upconverting NaYF4 nanocrystals doped with Er^{3+}, Yb^{3+} and Tm^{3+}, Yb^{3+} via thermal decomposition of lanthanide trifluoroacetate precursors," *J. Am. Chem. Soc.* **128**, 7444–7445 (2006).
51. K. A. Abel, J. C. Boyer, F. C. J. M. van Veggel, "Hard proof of the $NaYF_4$/$NaGdF_4$ nanocrystal core/shell structure," *J. Am. Chem. Soc.* **131**, 14644–14645 (2009).
52. N. Bogdan, F. Vetrone, G. A. Ozin, J. A. Capobianco, "Synthesis of ligand-free colloidally stable water dispersible brightly luminescent lanthanide-doped upconverting nanoparticles," *Nano Lett.* **11** (2), 835–840 (2011).
53. Z. Li, Y. Zhang, "An efficient and user-friendly method for the synthesis of hexagonal-phase $NaYF_4$: Yb, Er/Tm nanocrystals with controllable shape and upconversion fluorescence," *Nanotechnology* **19**, 345606 (2008).
54. C. Li, J. Lin, "Rare earth fluoride nano-/microcrystals: Synthesis, surface modification and application," *J. Mater. Chem.* **20**, 6831–6847 (2010).
55. G. S. Yi, G. M. Chow, "Synthesis of hexagonal-phase $NaYF_4$:Yb, Er and $NaYF_4$:Yb,Tm nanocrystals with efficient up-conversion fluorescence," *Adv. Funct. Mater.* **16**(18), 2324–2329 (2006).
56. J. Shan, Y. Ju, "A single-step synthesis and the kinetic mechanism for monodisperse and hexagonal-phase $NaYF_4$:Yb, Er upconversion nanophosphors," *Nanotechnology* **20**, 275603 (2009).
57. H. X. Mai, Y. W. Zhang, L. D. Sun, C. H. Yan, "Size- and phase-controlled synthesis of monodisperse $NaYF_4$:Yb, Er nanocrystals from a unique delayed nucleation pathway monitored with upconversion spectroscopy," *J. Phys. Chem. C* **111**, 13730–13739 (2007).
58. J. C. Boyer, L. A. Cuccia, J. A. Capobianco, "Synthesis of colloidal upconverting $NaYF_4$:Er^{3+}/Yb^{3+} and Tm^{3+}/Yb^{3+} monodisperse nanocrystals," *Nano Lett.* **7**(3), 847–852 (2007).
59. G. S. Yi, G. M. Chow, "Colloidal LaF_3:Yb, Er, LaF_3:Yb, Ho and LaF_3:Yb, Tm nanocrystals with multicolor upconversion fluorescence," *J. Mater. Chem.* **15**, 4460–4464 (2005).
60. G. Yi, H. Lu, S. Zhao, Y. Ge, W. Yang, D. Chen, L. H. Guo, "Synthesis, characterization, and biological application of size-controlled nanocrystalline $NaYF_4$:Yb, Er infrared-to-visible up-conversion phosphors," *Nano Lett.* **4**(11), 2191–2196 (2004).
61. Z. Li, Y. Zhang, "Monodisperse silica-coated polyvinylpyrrolidone/$NaYF_4$ nanocrystals with multicolor upconversion fluorescence emission," *Angew. Chem. Int. Ed.* **118**(46), 7896–7899 (2006).
62. G. Tian, Z. Gu, L. Zhou, W. Yin, X. Liu, L. Yan, S. Jin, W. Ren, G. Xing, S. Li, Y. Zhao, "Mn^{2+}

dopant-controlled synthesis of $NaYF_4$:Yb/Er upconversion nanoparticles for in vivo imaging and drug delivery," *Adv. Mater.* **24**(9), 1226–1231 (2012).
63. G. Wang, Q. Peng, Y. Li, "Upconversion luminescence of monodisperse CaF_2:Yb^{3+}/Er^{3+} nanocrystals," *J. Am. Chem. Soc.* **131**(40), 14200–14201 (2009).
64. X. Wang, J. Zhuang, Q. Peng, Y. Li, "A general strategy for nanocrystal synthesis," *Nature* **437** (7055), 121–124 (2005).
65. L. Wang, Y. Li, "Controlled synthesis and luminescence of lanthanide doped $NaYF_4$ nanocrystals," *Chem. Mater.* **19**(4), 727–734 (2007).
66. X. Liu, J. Zhao, Y. Sun, K. Song, Y. Yu, C. Du, X. Kong, H. Zhang, "Ionothermal synthesis of hexagonal-phase $NaYF_4$:Yb^{3+}, Er^{3+}/Tm^{3+} upconversion nanophosphors," *Chem. Commun.* **43**, 6628–6630 (2009).
67. A. Patra, C. S. Friend, R. Kapoor, P. N. Prasad, "Fluorescence upconversion properties of Er^{3+}-doped TiO_2 and $BaTiO_3$ nanocrystallites," *Chem. Mater.* **15**(19), 3650–3655 (2003).
68. F. Vetrone, J. C. Boyer, J. A. Capobianco, A. Speghini, M. Bettinelli, "Significance of Yb^{3+} concentration on the upconversion mechanisms in codoped Y_2O_3:Er^{3+}, Yb^{3+} nanocrystals," *J. Appl. Phys.* **96** (1), 661–667 (2004).
69. X. Qin, T. Yokomori, Y. Ju, "Flame synthesis and characterization of rare-earth (Er^{3+}, Ho^{3+}, and Tm^{3+}) doped upconversion nanophosphors," *Appl. Phys. Lett.* **90**, 073104 (2007).
70. R. B. Liebherr, T. Soukka, O. S. Wolfbeis, H. H. Gorris, "Maleimide activation of photon upconverting nanoparticles for bioconjugation," *Nanotechnology* **23**, 485103 (2012).
71. H. Schafer, P. Ptacek, K. Kompe, M. Haase, "Lanthanide-doped $NaYF_4$ nanocrystals in aqueous solution displaying strong up-conversion emission," *Chem. Mater.* **19**(6), 1396–1400 (2007).
72. Q. Zhang, K. Song, J. Zhao, X. Kong, Y. Sun, X. Liu, Y. Zhang, Q. Zeng, H. Zhang, "Hexanedioic acid mediated surface-ligand-exchange process for transferring $NaYF_4$:Yb/Er (or Yb/Tm) up-converting nanoparticles from hydrophobic to hydrophilic," *J. Colloid Interf. Sci.* **336**(1), 171–175 (2009).
73. L. Xiong, Y. Tianshe, Y. Yang, C. Xu, F. Li, "Long-term in vivo biodistribution imaging and toxicity of polyacrylic acid-coated upconversion nanophosphors," *Biomaterials* **31**(27), 7078–7085 (2010).
74. N. J. J. Johnson, N. M. Sangeetha, J. C. Boyer, F. C. J. M. van Veggel, "Facile ligand-exchange with polyvinylpyrrolidone and subsequent silica coating of hydrophobic upconverting β-$NaYF_4$: Yb^{3+}/Er^{3+} nanoparticles," *Nanoscale* **2**, 771–777 (2010).
75. Z. Chen, H. Chen, H. Hu, M. Yu, F. Li, Q. Zhang, Z. Zhou, T. Yi, C. Huang, "Versatile synthesis strategy for carboxylic acid-fucntionalized upconverting nanophosphors as biological labels," *J. Am. Chem. Soc.* **130**(10), 3023–3029 (2008).
76. H. P. Zhou, C. H. Xu, W. Sun, C. H. Yan, "Clean and flexible modification strategy for carboxyl/aldehyde-functionalized upconversion nanoparticles and their optical applications," *Adv. Funct. Mater.* **19**(24), 3892–3900 (2009).
77. S. J. Budijono, J. Shan, N. Yao, Y. Miura, T. Hoye, R. H. Austin, Y. Ju, R. K. Prud'homme, "Synthesis of stable block-copolymer-protected $NaYF_4$:Yb^{3+}, Er^{3+} up-converting phosphor nanoparticles," *Chem. Mater.* **22**(2), 311–318 (2010).
78. L. L. Li, R. Zhang, L. Yin, K. Zheng, W. Qin, P. R. Selvin, Y. Lu, "Biomimetic surface engineering of lanthanid-doped upconversion nanoparticles as versatile bioprobes," *Angew. Chem.* **124**(25), 6225–6229 (2012).
79. C. F. Gainer, U. Utzinger, M. Romanowski, "Scanning two-photon microscopy with upconverting lanthanide nanoparticles via Richardson-Lucy deconvolution," *J. Biomed. Opt.* **17**(7), 076003 (2012).
80. H. Kobayashi, N. Kosaka, M. Ogawa, N. Y. Morgan, P. D. Smith, C. B. Murray, X. Ye, J. Collins, A. G. Kumar, H. Bell, P. L. Choyke, "In vivo multiple color lymphatic imaging using upconverting nanocrystals," *J. Mater. Chem.* **19**, 6481–6484 (2009).
81. R. A. Jalil, Y. Zhang, "Biocompatibility of silica coated $NaYF_4$ upconversion fluorescent nanocrystals," *Biomaterials* **29**(30), 4122–4128 (2008).
82. J. Shan, Y. Ju, "Controlled synthesis of lanthanide-doped $NaYF_4$ upconversion nanocrystals via ligand induced crystal phase transition and silica coating," *Appl. Phys. Lett.* **91**(12), 123103 (2007).
83. H. S. Choi, W. Liu, P. Misra, E. Tanaka, J. P. Zimmer, B. I. Ipe, M. G. Bawendi, J. V. Frangioni, "Renal clearance of nanoparticles," *Nat. Biotechnol.* **25**(10), 1165–1170 (2007).
84. E. M. Chan, G. Han, J. D. Goldberg, D. J. Gargas, A. D. Ostrowski, J. P. Schuck, B. E. Cohen, D. J. Milliron, "Combinatorial discovery of lanthanide–doped nanocrystals with spectrally pure upconverted emission," *Nano Lett.* **12**(7), 3839–3845 (2012).